Modulational instability and exact solutions of the discrete cubic–quintic Ginzburg–Landau equation

R Murali[1]**, K Porsezian**[1]**, T C Kofané**[2]** and A Mohamadou**[2]

[1] Department of Physics, School of Physical, Chemical and Applied Sciences, Pondicherry University, Puducherry-605 014, India
[2] Laboratory of Mechanic, Department of Physics, Faculty of Sciences, The University of Yaoundé I, PO Box 812, Yaoundé, Cameroon

E-mail: muralipu@rediffmail.com, ponzsol@yahoo.com, tkofane@uycdc.uninet.cm and mohdoufr@yahoo.fr

Abstract

In this paper, we investigate analytically and numerically the modulational instability in a model of nonlinear physical systems such as Bose–Einstein condensates in a deep optical lattice. This model is described by the discrete complex cubic–quintic Ginzburg–Landau equation with a non-local quintic term. We obtain characteristics of the modulational instability in the form of typical dependences of the instability growth rate (gain) on the perturbation wavenumber and the system's parameters. Excellent agreement has been obtained between the analytical and numerical study. Further, we derive the periodic function and new type of solitary wave solutions for the above system. By using the extended Jacobi elliptic function approach, we obtain the exact stationary solitons and periodic wave solutions of this equation. These solutions include the Jacobi periodic wave solution, alternating phase Jacobi periodic wave solution, kink and bubble soliton solutions, alternating phase kink soliton and alternating phase bubble soliton solutions.

PACS numbers: 74.20.De, 03.75.Lm

1. Introduction

Complex Ginzburg–Landau (CGL) equations are universal models describing the formation of nonlinear dissipative patterns, which find direct applications in nonlinear optics, hydrodynamics, superconductivity, chemical waves, etc [1]. The CGL equation was originally introduced with linear gain and cubic nonlinear loss. This equation gives rise to exact solutions for solitary pulses [2], but they are unstable. The most straightforward way to modify the equation so as to facilitate the existence of stable pulses is to introduce the cubic–quintic nonlinearity, with *linear loss* and *cubic gain*, supplemented by a quintic loss term to secure

the overall stability of the model. The complex cubic–quintic Ginzburg–Landau (CCQGL) equation was originally proposed by Sergeev and Petviashvili [3], and stable solitary pulses in this model were first predicted in [4]. Later, solutions of the CCQGL equation were investigated by many authors in great detail [5].

In recent years, discrete solitons have been investigated in many diverse branches of physical systems such as Bose–Einstein condensates (BECs) [6], optical waveguide arrays [7], solid state physics [8] and photonic crystal structures [9]. The two-dimensional discrete solitons have been observed in nonlinear photonic lattice [10]. The dynamical and structural stability of the discrete breathers have been discussed in detail for various nonlinear physical systems [11]. Recently, discrete breathers have also been reported in an array of BECs [12]. By using the extended Jacobi elliptic function approach, the exact periodic and solitary wave solutions have been constructed for the discrete nonlinear Schrödinger equation with non-local cubic and quintic nonlinear terms [13]. Discrete CGL equation models have also been studied in the literature [14]. Maruno *et al* have derived a set of exact solutions for the discrete complex cubic Ginzburg–Landau equation which includes periodic, bright and dark soliton solutions [15].

The stability of the open BEC has been discussed under the influence of the real and imaginary parts of the two-body interaction effect [16]. Recently, modulational instability (MI) and the properties of discrete breathers have been investigated for the system of BECs in optical lattice with the influence of the real part of the three-body interactions [17–19]. The dynamics of growth and collapse of BECs have been discussed in detail with an imaginary part of three-body interaction, i.e. dissipation loss term [20]. With these studies of higher order interactions having been already reported individually in real and imaginary domains separately, we have now analyzed the modulational instability and found the exact periodic and soliton solutions in BECs in a deep optical lattice with the inclusion of the complex form of cubic (two-body interaction) and quintic (three-body interaction) nonlinear terms. We consider a one-dimensional BEC in deep optical lattice described by the following discrete complex cubic–quintic Ginzburg–Landau (DCCQGL) equation [21–23]:

$$
i\frac{\partial \psi_n}{\partial t} + (\alpha - i\beta)(\psi_{n+1} + \psi_{n-1} - 2\psi_n) + (\sigma - i\epsilon)|\psi_n|^2\psi_n + (\nu - i\lambda)|\psi_n|^4\psi_n - i\gamma\psi_n = 0,
$$

(1)

where all nonlinear terms are local in nature. High atomic density of the BEC in the optical lattice implies that the effect due to the interatomic interactions can become important. The most prominent effect associated with the periodicity of the lattice is the boson tunneling from one well to the next [24]. With this effect, the BEC atoms are confined in an array of optical traps, and the tunneling among the BECs confined in the multiwell potential has been observed in [25]. In equation (1), ψ_n represents the complex wave function at site n. Physically, the coefficient α accounts for the energy tunneling between adjacent elements of the lattice, while the imaginary term β stands for gain (loss) due to the coupling between neighboring sites of the optical lattice. In general, the cubic and quintic nonlinearity coefficients are complex quantities. The real parts of the cubic and quintic nonlinearity coefficients σ and ν correspond to the two- and three-body elastic collisions in the condensates. The coefficient σ satisfies the following conditions: $\sigma > 0$ corresponds to the repulsive interaction and $\sigma < 0$ represents an attractive interaction case. Next, the imaginary part of the cubic and quintic nonlinearity coefficients ϵ and λ appears due to two- and three-body inelastic collisions in the condensates [18, 26]. Finally, the coefficient γ indicates the linear loss/gain parameter due to the feeding strength from the thermal clouds of the condensates. When $\beta = \epsilon = \nu = \lambda = \gamma = 0$, equation (1) is reduced to the (non-integrable) discrete nonlinear Schrödinger equation [27].

The MI and pattern formation have been discussed in the discrete dissipative system described by the DCCQGL equation with local cubic and quintic nonlinear terms [21]. By using the perturbation technique, Abdullaev *et al* found the soliton solution for the DCCQGL equation with non-local cubic and local quintic nonlinear terms which is valid at small values of the dissipative terms for this equation [22]. In [23], the discrete soliton has been analyzed for the DCCQGL equation having several features that have no counterparts in either continuous limit or other conservative discrete models.

When the quintic nonlinear term is dropped in equation (1), the cubic nonlinear equation is shown to exhibit a lack of stable solutions, except in very special cases [28]. In the case of a cubic nonlinear equation, after a certain distance of propagation the soliton either collapses or disappears. Stability can be achieved if we add quintic terms to the system. In physics problems, the quintic nonlinearity can be equal to or even more important than the cubic one [28] as it is responsible for more stability of localized solutions. Note that in our system of BECs, the quintic mean-field nonlinearity corresponds to the three-body interaction effects which occur only when the density of BECs in optical lattice is increased. The existence of three-body interactions can play an important role in terms of condensate stability [26, 29]. Hence, the nonlocal quintic term plays a crucial role in the system of BEC in a deep optical lattice when the interaction is between the boson and the next-nearest-neighboring bosons. The exact solutions for the DCCQGL equation with the non-local quintic term of lowest order responsible for the dissipation which are mainly different from the approximate solutions obtained for the DCCQGL equation with the local quintic term with the dissipative term being small have been proposed [30]. In the same way, the exact soliton and periodic solutions for the DCCQGL equation with the non-local quintic term of lowest order for the dynamics of the BEC under the influence of the strong three-body collisions are dissimilar from the approximate solutions for the DCCQGL equation with the local quintic nonlinear term. Therefore, the exact stable solution can be achieved by changing the non-local quintic term instead of local quintic in equation (1). Then, the DCCQGL equation with the non-local quintic term is as follows [30, 31]:

$$
i\frac{\partial \psi_n}{\partial t} + (\alpha - i\beta)(\psi_{n+1} + \psi_{n-1} - 2\psi_n) + (\sigma - i\epsilon)|\psi_n|^2\psi_n
$$
$$
+ (\nu - i\lambda)|\psi_n|^4(\psi_{n+1} + \psi_{n-1}) - i\gamma\psi_n = 0. \tag{2}
$$

The quintic nonlinear term in equation (2) represents the non-local term which is different from the system studied in [22, 23]. The dissipative soliton has been investigated for the DCCQGL equation with the non-local quintic term [30]. The continuum limit of equation (1) is the CCQGL equation [32]:

$$
i\frac{\partial \psi}{\partial t} + (\alpha - i\beta)\frac{\partial^2 \psi}{\partial x^2} + (\sigma - i\epsilon)|\psi|^2\psi + (\nu - i\lambda)|\psi|^4\psi - i\gamma\psi = 0. \tag{3}
$$

Equation (3) is applicable to many physically realizable systems such as superconductivity and superfluidity [33], non-equilibrium fluid dynamics [34], chemical systems [35], nonlinear optics [36, 37], BECs [16], etc.

Note that the exact solutions of equation (2) have been derived by using the extended tanh-function approach [31]. In this paper, we derive the new form of exact periodic and soliton solutions of equation (2) by using the extended Jacobi elliptic function approach. The paper is organized as follows. In section 2, we present the scheme of the linear stability analysis. The results and discussions of the MI analysis are also presented and also our analytical results are verified through numerical methods. Furthermore, the new form of exact (periodic and new type of soliton) solutions are also carried out for the underlying equations in section 3. The conclusion is presented in section 4.

2. Modulational instability

Recently, the MI and pattern formation have been reported for the discrete dissipative system governed by equation (1) [21]. In recent times, the dynamics and stability of BECs trapped in a deep one-dimensional periodic optical lattice with the elastic properties of the two- and three-body interactions have been reported in [38]. In this section, we analyze instabilities of BECs trapped in an optical lattice with elastic and inelastic properties of the two- and three-body interactions including feeding of the condensates term, which is described by equation (2). The aim of the stability analysis is to perturb the system slightly and then study whether this small perturbation grows or decays with propagation. Now, we proceed to discuss the occurrence of MI for the considered system. The plane wave solution to equation (2) with constant amplitude, A, is

$$\psi_n = A\, e^{i(qn-\omega t)}, \tag{4}$$

where q and ω are the wavenumber and frequency, respectively. Substituting equation (4) in equation (2), we obtain the nonlinear dispersion relation

$$\omega = 2\alpha - \sigma A^2 - 2\cos(q)[\alpha + \nu A^4] \tag{5}$$

$$A^2 = \frac{-\epsilon \,\pm\, \sqrt{\epsilon^2 + 8\lambda \cos(q)(2\beta - 2\beta \cos(q) - \gamma)}}{4\lambda \cos(q)}. \tag{6}$$

The initial amplitude of the plane wave solution (6) is different compared with the equation (2) in [21]. Without the nonlocal term, the stability of the plane wave solution is strongly affected by the dissipative loss parameter [21]. Also, in [21] the stability of the system is analyzed in general and not widely discussed for the different physical conditions of the carrier wavenumber $q = 0, \pi$ and $\pi/2$. In [21], we considered the first two values of q $(0, \pi)$ where the stability of the plane wave solution is strongly affected by the dissipative loss parameter. Also, the instability gain of the plane wave solution is determined for $q = \pi/2$. To the best of our knowledge, these discussions are entirely different under the influence of a nonlocal term. In this section, we discus the stability of the amplitude modulation of the plane wave solution for different values of the carrier wavenumber q under the influence of the nonlocality in detail. To analyze the MI of plane wave solutions (4), we perturb them by introducing

$$\psi_n = (A + \phi_n)\, e^{i(qn-\omega t)}, \tag{7}$$

where ϕ_n is an infinitesimal complex perturbation which obeys the following linearized equations,

$$i\frac{\partial \phi_n}{\partial t} + (\alpha + \sigma A^4)[\cos(q)(\phi_{n+1} + \phi_{n-1}) + i\sin(q)(\phi_{n+1} - \phi_{n-1})]$$
$$- 2\alpha \cos(q)\phi_n + 2\sigma A^4 \cos(q)(\phi_n + 2\phi_n^*) + \eta A^2(\phi_n + \phi_n^*) = 0, \tag{8}$$

where ϕ_n^* is the complex conjugate. The modulational perturbation is taken in the ordinary form,

$$\phi_n = \phi_1\, e^{i(Qn-\Omega t)} + \phi_2^*\, e^{-i(Qn-\Omega^* t)}, \tag{9}$$

where Q and Ω are, respectively, an arbitrary wavenumber and the corresponding frequency of the perturbation. Substituting equation (9) into equation (8), we obtain the matrix form for the set of homogeneous equations for ϕ_1 and ϕ_2:

$$\begin{pmatrix} m_{11} - i\Omega & m_{12} \\ m_{21} & m_{22} - i\Omega \end{pmatrix} \begin{pmatrix} \phi_1 \\ \phi_2 \end{pmatrix} = 0. \tag{10}$$

The coefficients of the 2×2 matrix (m_{ij}) are given in the appendix. The dispersion relation, which determines Ω as a function of Q, is obtained from the solvability condition of the homogeneous matrix equation when its determinant of the coefficient matrix vanishes. Finally, we obtain the dispersion relation of the amplitude modulation of the plane wave as

$$\Omega^2 + i\Omega(m_{11} + m_{22}) + m_{12}m_{21} - m_{11}m_{22} = 0. \tag{11}$$

Since the dispersion relation (11) is complex, then the instability of the system is defined by the imaginary part of $\Omega(Q)$, i.e. $G \equiv |\text{Im}(\Omega(Q))|$. It should be noted that the presence of a trigonometric function in the dispersion relation (11) makes a main difference between the continuous and discrete systems. From equation (11), we analyze the condition of the MI gain for the unstaggered (large wavelength limit) and staggered (short wavelength limit) cases about the carrier wavenumber q for both attractive and repulsive condensates as follows.

2.1. Large wavelength limit

First, we consider the unstaggered (large wavelength limit) case when the carrier wavenumber $q = 0$; the linear property of equation (11) in q explains that the BEC system supports the sound waves which propagate on the top of the plane wave $\psi_n = A\,e^{i(qn-\omega t)}$. According to this condition of q, the values of $\sin(q) = 0$, $\cos(q) = 1$ and hence the solutions of the dispersion relation (11) are

$$\Omega_\pm|_{q=0} = U_{q=0} \pm \sqrt{X_1 - X_2 - X_3}, \tag{12}$$

where $U_{q=0} = \epsilon A^2 - 2(\beta - \lambda A^4) + 2(\beta + \lambda A^4)\cos(Q)$, $X_1 = 2\epsilon^2 A^4 + 16\epsilon\lambda A^6 + 32\lambda^2 A^8$, $X_2 = 8[\sigma A^2(\alpha + \nu A^4) - 2(\alpha^2 - \nu^2 A^8)](\cos(Q) - 1)$, $X_3 = 8[\alpha^2 + \nu^2 A^8 + 2\alpha\nu A^4](\cos^2(Q) - 1)$ and $A^2 = \frac{1}{4\lambda}\left(-\epsilon \pm \sqrt{8\lambda[(\gamma_{cr})_{q=0} - \gamma]}\right)$ with $(\gamma_{cr})_{q=0} = \frac{\epsilon^2}{8\lambda}$. It is interesting to mention here that when the imaginary part of the three-body interaction coefficient $\lambda \to 0$, the amplitude of the carrier wave $A \to \infty$. Then the three-body inelastic collision will play a crucial role in the dispersion relation (12). From the dispersion relation (12), the MI gain relation can be written as

$$G_{q=0} = |\text{Im}(\Omega_\pm|_{q=0})| = \sqrt{X_3 + X_2 - X_1}. \tag{13}$$

In the large wavelength limit, the dispersion relation (12) contains the dissipative loss parameter β while the gain relation (13) does not include β, which means that the stability of the plane wave solution becomes unaffected by the dissipative loss parameter β due to the crucial role of the nonlocal term. For the unstaggered (large carrier wavelength limit) case, the amplitude modulation of the plane wave solution is unstable for the following two conditions: (i) $\gamma < (\gamma_{cr})_{q=0}$, $\lambda > 0$ and the gain region can be defined by

$$\cos(Q) > \frac{2\alpha^2 - \sigma\alpha A^2 - \nu A^6(\sigma + 2\nu A^2) - \sqrt{M}}{2(\alpha + \nu A^4)^2} \quad \text{for} \quad \sigma > 0, \tag{14}$$

$$\cos(Q) < \frac{2\alpha^2 - \sigma\alpha A^2 - \nu A^6(\sigma + 2\nu A^2) - \sqrt{M}}{2(\alpha + \nu A^4)^2} \quad \text{for} \quad \sigma < 0. \tag{15}$$

(ii) $\gamma > (\gamma_{cr})_{q=0}$, $\lambda < 0$, and the conditions of $\cos(Q)$ are exactly exchanged for σ conditions as compared with the previous conditions of the gain region, where $M = A^4(\alpha + \nu A^4)^2(\epsilon^2 + 8\epsilon\lambda A^2 + 16A^4\{\nu^2 + \lambda^2\} + 8\sigma\nu A^2 + \sigma^2)$. Figure 1 portrays the MI gain spectra for the unstaggered condition wherein the two above-mentioned conditions are satisfied. The solid line corresponds to a repulsive condensate when the strength of the nonlinear coefficient
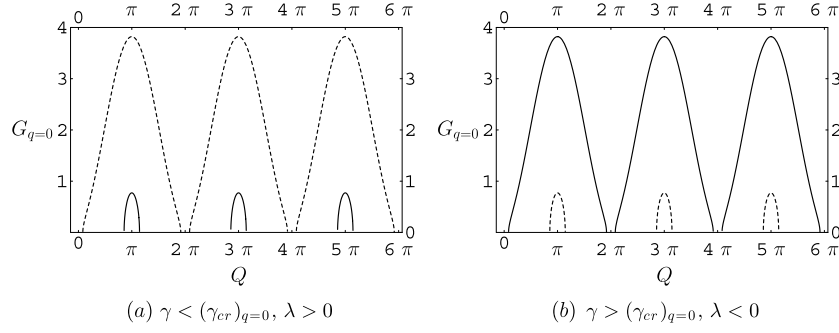
Figure 1. Instability gain spectrum for the unstaggered condition ($q = 0$) when (*a*) $\lambda = 0.25$ and $\gamma = 0.1$; (*b*) $\lambda = -0.25$ and $\gamma = -0.1$. The solid line corresponds to a repulsive condensate when $\sigma = 1$. The dashed line corresponds to an attractive condensate when $\sigma = -1$. Other physical parameter values are $\alpha = 0.5$, $\epsilon = -0.5$ and $\nu = 0.2$.

$\sigma = 1$ and the dashed line corresponds to an attractive case for $\sigma = -1$. Considering the first period between 0 and 2π in figure 1(*a*), the MI gain for $\gamma < (\gamma_{cr})_{q=0}$, $\lambda > 0$ occurs only in the negative region of $\cos(Q) > 0.8987$ for the repulsive condensate (solid line) and $\cos(Q) < 0.9666$ for the attractive condensate (dashed line) when the strength of the feeding term is positive, which is clearly seen in figure 1(*a*). The scenario of MI gain for the second condition as $\gamma > (\gamma_{cr})_{q=0}$, $\lambda < 0$, gets exactly reversed which is clearly portrayed in figure 1(*b*). When the value of perturbed wavenumber $Q = (2n + 1)\pi$ ($n = 0, 1, 2, \ldots$), the optimum instability gain can be calculated by

$$(G_{\text{opt}})_{q=0} = [2(16\alpha^2 - 8\sigma\alpha A^2 - \epsilon^2 A^4 - 8(\epsilon\lambda + \nu\sigma)A^6 - 16(\lambda^2 + \nu^2)A^8)]^{\frac{1}{2}}. \tag{16}$$

2.2. Short wavelength limit

Next, we consider the staggered case when $q = \pi$; the linear property of equation (11) in q explains that the BEC system supports the unsteady sound waves which propagate on the top (n is even) of the plane wave $\psi_n = A\,\mathrm{e}^{\mathrm{i}(qn - \mu t)}$ or at the bottom (n is odd) of the plane wave. For this above-mentioned condition of q, the values of $\sin(q) = 0$, $\cos(q) = -1$ and hence the solutions of the dispersion relation (11) are as follows:

$$\Omega_{\pm}|_{q=\pi} = U_{q=\pi} \pm \sqrt{Y_1 + Y_2 - Y_3}, \tag{17}$$

where $U_{q=\pi} = \epsilon A^2 + 2(\beta - \lambda A^4) - 2(\beta + \lambda A^4)\cos(Q)$, $Y_1 = 2\epsilon^2 A^4 - 16\epsilon\lambda A^6 + 32\lambda^2 A^8$, $Y_2 = 8[\sigma A^2(\alpha + \nu A^4) + 2(\alpha^2 - \nu^2 A^8)](\cos(Q) - 1)$, $Y_3 = X_3$ and $A^2 = \frac{1}{4\lambda}(-\epsilon \pm \sqrt{8\lambda[\gamma - (\gamma_{cr})_{q=\pi}]})$ with $(\gamma_{cr})_{q=\pi} = 4\beta - \frac{\epsilon^2}{8\lambda}$. From relation (17), we obtain the MI gain relation for the staggered case as follows:

$$G_{q=\pi} = |\mathrm{Im}(\Omega_{\pm}|_{q=\pi})| = \sqrt{Y_3 - Y_2 - Y_1}. \tag{18}$$

For the short wavelength limit, the dispersion relation (17) and the gain relation (18) depend on the dissipative loss parameter (β). For this reason, the instability condition of the amplitude modulation of the plane wave solution is strongly affected by the influence of the dissipative loss parameter β. In the staggered (short carrier wavelength limit) case, the amplitude modulation of the plane wave solution is unstable for the following two different conditions:
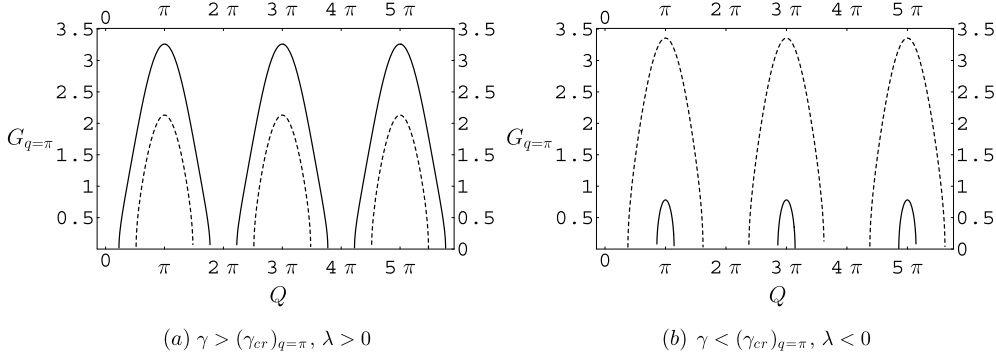
Figure 2. Instability gain spectrum for the staggered condition ($q = \pi$) when (*a*) $\lambda = 0.5$ and $\gamma = 0.05$; (*b*) $\lambda = -0.5$ and $\gamma = 0.05$. The solid and dashed lines correspond to the repulsive ($\sigma = 1$) and attractive $\sigma = -1$ condensates, respectively. Other physical parameter values are $\alpha = 0.5$, $\beta = 0.025$, $\epsilon = -0.5$ and $\nu = 0.2$.

(i) $\gamma > (\gamma_{cr})_{q=\pi}$, $\lambda > 0$ and the region of the MI gain can be described by

$$\cos(Q) < \frac{2\alpha^2 + \sigma\alpha A^2 + \nu A^6(\sigma - 2\nu A^2) - \sqrt{N}}{2(\alpha + \nu A^4)^2} \quad \text{for} \quad \sigma > 0, \quad (19)$$

$$\cos(Q) > \frac{2\alpha^2 + \sigma\alpha A^2 + \nu A^6(\sigma - 2\nu A^2) - \sqrt{N}}{2(\alpha + \nu A^4)^2} \quad \text{for} \quad \sigma < 0. \quad (20)$$

(ii) $\gamma < (\gamma_{cr})_{q=\pi}$, $\lambda < 0$, and the conditions of $\cos(Q)$ are exactly exchanged for σ conditions as compared with the previous condition, where $N = A^4(\alpha + \nu A^4)^2(\epsilon^2 - 8\epsilon\lambda A^2 + 16A^4\{\nu^2 + \lambda^2\} - 8\sigma\nu A^2 + \sigma^2)$. Figure 2 depicts the MI gain spectra for repulsive (solid line when $\sigma = 1$) and attractive (dashed line when $\sigma = -1$) condensates for the staggered condition when $q = \pi$. Now, we choose the one period between 0 and 2π in figure 2(*a*); the MI gain for $\gamma > (\gamma_{cr})_{q=\pi}$, $\lambda > 0$ occurs only when $\cos(Q) < 0.7578$ for a repulsive condensate (solid line) and in the negative region of $\cos(Q) > 0.0545$ for an attractive condensate (dashed line) which is clearly seen in figure 2(*a*). We observe from figure 2(*b*) that the MI gain for $\gamma < (\gamma_{cr})_{q=\pi}$, $\lambda < 0$ arises only in the negative region of $\cos(Q) > 0.9011$ for a repulsive case and $\cos(Q) < 0.3710$ for an attractive one. When $Q = (2n + 1)\pi$ ($n = 0, 1, 2, \ldots$), the optimum instability gain can be written as

$$(G_{\text{opt}})_{q=\pi} = [2(16\alpha^2 + 8\sigma\alpha A^2 - \epsilon^2 A^4 + 8(\epsilon\lambda + \nu\sigma)A^6 - 16(\lambda^2 + \nu^2)A^8)]^{\frac{1}{2}}. \quad (21)$$

In the high atomic density case, the three-body interaction is more dominant than the two-body interaction. Then the cubic nonlinear coefficients take the values $\sigma = \epsilon = 0$. Hence, the stability of BEC in optical lattice is controlled by the three-body interactions. For the unstaggered case ($q = 0$), the MI can occur for the following two conditions: (i) $\gamma < 0$, $\lambda > 0$, (ii) $\gamma > 0$, $\lambda < 0$, otherwise stable. Next, we consider the staggered case ($q = \pi$). If $\lambda > 0$, we have MI when $\gamma > 4\beta$ and if $\lambda < 0$, then we have MI when $\gamma < 4\beta$, otherwise stable.

Finally, we consider the value of the carrier wavenumber $q = \pi/2$; then $\sin(q) = 1$, $\cos(q) = 0$ but $A^2 \to \infty$, and hence the dispersion relation $\Omega_{q=\frac{\pi}{2}} \to \infty$. Then the instability of the plane wave solution cannot be determined, i.e. the plane wave solution is always stable for the above-mentioned condition. In the absence of nonlocality [21], the stability of the plane wave solution is affected when $q = \pi/2$.
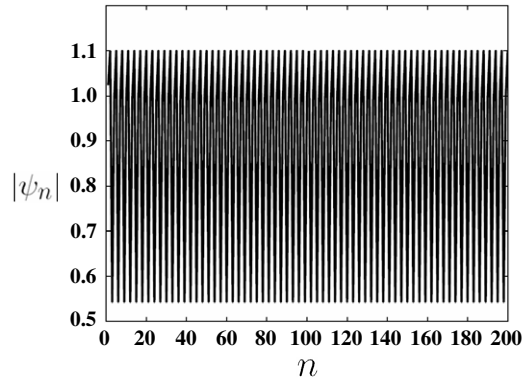
Figure 3. Propagation of stable patterns though the system at time 300 units induced by the modulational instability. Other physical parameter values are $q = 5\pi/3$, $Q = 2\pi/3$, $\alpha = 0.5$, $\beta = 0.2$, $\sigma = 1$, $\nu = 2/3$, $\epsilon = \lambda = -0.7$ and $\gamma = 2$.

2.3. Numerical results

Linear stability analysis can determine the instability domain in parameter space and predict quantitatively how the amplitude of the modulation sideband evolves at the onset of instability. However, such analysis is based on the linearization around the unperturbed carrier wave, which is valid only when the amplitude of perturbation is small in comparison with that of the carrier wave. Clearly, the linear approximation must fail at large time scales as the amplitude of the unstable sideband grows exponentially. In order to check the validity of our analytical analysis and to investigate the longtime evolution of the modulated nonlinear wave, we have carried out numerical investigations of MI on the DCCQGL equation (2). Equation (2) has been integrated with a fourth-order Runge–Kutta scheme, with the given initial condition (6), and periodic boundary conditions [39, 40].

Let us consider the case $\phi_1 = \phi_2 = 0.1$, $q = 5\pi/3$, $Q = 2\pi/3$, $\gamma = 2$, $\alpha = 1/2$, $\beta = 0.2$, $\sigma = 1$, $\nu = 2/3$ and $\varepsilon = \lambda = -0.7$. The initial excitation moves without changing its form as coherent states. The wave pattern displayed by the set of the preceding parameters' system is that of a plane wave with a sinusoidal form, with a constant amplitude that is not sensitive to any modulation as the time increases. Therefore, the system is said to be stable under the corresponding modulation. This feature is described in figure 3 at time 300 units.

As a second case, let us consider $\phi_1 = \phi_2 = 0.01$, $q = 5\pi/3$, $Q = 5\pi/4$, $\gamma = 2$, $\alpha = 0.5$, $\beta = 0.2$, $\varepsilon = 2/3$ and $\lambda = \nu = -0.7$. For this value of parameters, the initial condition is introduced in the system. One obtains an interesting phenomenon: the wave displays an oscillating and breathing wave behavior. The amplitude of the wave generated by wave motion is modulated in the form of a train of small amplitude with short wavelength. Figure 4(*a*) presents such a phenomenon at time 300 units. From the parameters of figure 4(*b*), we now consider $q = \pi/3$ and $Q = 5\pi/8$. We have observed that the wavelength of each wave packet slightly increases but their number decreases. Each component of the train of the wave depicted in figure 4(*b*) has the shape of a soliton-like object. One can conclude that the value of the wavenumber of modulation influences the number of waves oscillating with a soliton-like shape in the train. It is interesting to note that, at the staggered (short wavelength) condition, the matter wave soliton train of oscillatory form can be generated in the optical lattice by a small perturbation of the plane wave solution which is clearly demonstrated in figure 4(*b*). One can also add that this type of evolution is typical for modulationally unstable
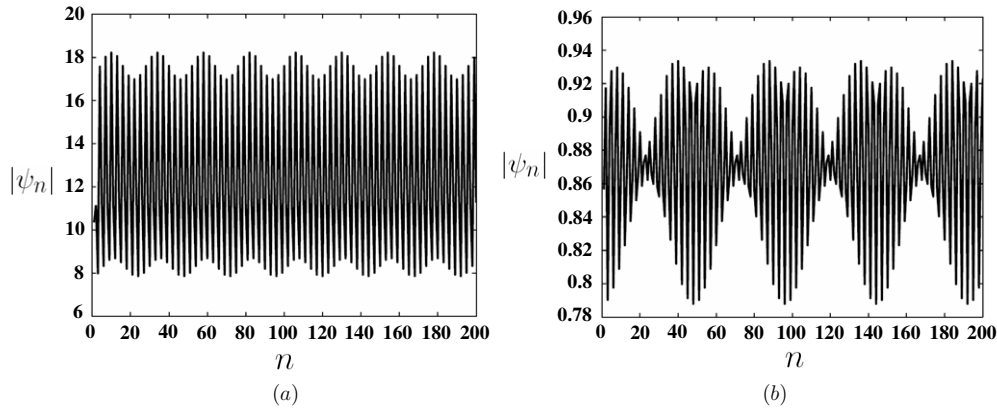
Figure 4. Propagation of unstable patterns though the system at time 300 units induced by the modulational instability. Other physical parameter values are $\alpha = 0.5$, $\beta = 0.2$, $\epsilon = 2/3$, $\nu = \lambda = -0.7$, $\gamma = 2$ for (*a*) the small amplitude periodic pattern when $q = 5\pi/3$, $Q = 5\pi/4$; (*b*) matter wave soliton train-like pattern when $q = \pi/3$, $Q = 5\pi/8$.

discrete systems, and has been observed in numerous publications dealing with MI in similar systems from Kivshar and Peyrard's work onwards [40, 41].

It is well known that MI is a fundamental mechanism that leads to the formation of localized solitary-wave structures in a variety of settings. The most standard mechanism through which bright solitons and solitary wave structures appear is the activation of the MI of plane wave (see figure 4). Since the disintegration of figure 4 typically occurs in the same parameter region where bright solitons are observed, MI is considered to some extent a precursor to soliton formation. So, the next section will be dedicated to deriving such solutions.

3. Exact solutions of the DCCQGL equation

Recently, the exact periodic and soliton solutions have been derived for the DCCQGL equation by using the extended tanh-function approach [31]. In this section, we are interested in deriving the new form of periodic and soliton solutions for the DCCQGL equation by using the extended Jacobi elliptic function approach. Now, we achieve the exact solution of the DCCQGL equation under the following transformations:

$$\psi_n = e^{i\theta_n} V_n(\rho_n), \tag{22}$$

where $\rho_n = un + ct + \delta_1$ and $\theta_n = rn + st + \delta_2$. We can also write $\psi_{n\pm1} = e^{i\theta_n} e^{\pm ir} V_{n\pm1}(\rho_{n\pm1})$ with $\rho_{n\pm1} = \rho_n \pm u$. Substituting equation (22) into equation (2), and separating the real and imaginary parts, we obtain

$$
\begin{aligned}
\left(\alpha + \nu V_n^4\right)\cos(r)(V_{n+1} + V_{n-1}) &+ \left(\beta + \lambda V_n^4\right)\sin(r)(V_{n+1} - V_{n-1}) \\
&- (2\alpha + s)V_n + \sigma V_n^3 = 0,
\end{aligned}
\tag{23}
$$

$$
\begin{aligned}
cV_n' - \left(\beta + \lambda V_n^4\right)\cos(r)(V_{n+1} + V_{n-1}) &+ \left(\alpha + \nu V_n^4\right)\sin(r)(V_{n+1} - V_{n-1}) \\
&+ (2\beta - \gamma)V_n - \epsilon V_n^3 = 0,
\end{aligned}
\tag{24}
$$

9

where $V_n \equiv V_n(\rho_n)$, $V_{n+1} \equiv V_{n+1}(\rho_{n+1})$, $V_{n-1} \equiv V_{n-1}(\rho_{n-1})$ and $V_n' = \frac{\partial V_n}{\partial t}$. The solution of equations (23) and (24) in terms of the series expansion of the Jacobi elliptic function is given by [13]

$$V_n(\rho_n) = \mu_0 + \mu_1 \operatorname{sn}(\rho_n) + \mu_2 \operatorname{sn}^2(\rho_n). \tag{25}$$

Similarly, we can write $V_{n\pm1}(\rho_{n\pm1}) = \mu_0 + \mu_1 \operatorname{sn}(\rho_{n\pm1}) + \mu_2 \operatorname{sn}^2(\rho_{n\pm1})$, where $\operatorname{sn}(\rho_n)$, $\operatorname{sn}(\rho_{n+1})$ and $\operatorname{sn}(\rho_{n-1})$ are the standard Jacobi elliptic functions with the modulus m ($0 < m < 1$). In this paper, we utilize both cnoidal and solitary wave theories to investigate the dynamical evolution of BECs. By using the addition property of the Jacobi elliptic function, the values of $\operatorname{sn}(\rho_{n+1})$ and $\operatorname{sn}(\rho_{n-1})$ can be written as

$$\operatorname{sn}(\rho_{n\pm1}) = \operatorname{sn}(\rho_n \pm u) = \frac{\operatorname{sn}(\rho_n)\operatorname{cn}(u)\operatorname{dn}(u) \pm \operatorname{sn}(u)\operatorname{cn}(\rho_n)\operatorname{dn}(\rho_n)}{1 - m^2 \operatorname{sn}^2(\rho_n)\operatorname{sn}^2(u)}. \tag{26}$$

Substituting equations (25) and (26) into equations (23) and (24), we obtain a series of over-determined algebraic equations by eliminating the denominator and setting the coefficients of all powers like $\operatorname{sn}^i(\rho_n)$ ($i = 0, 1, 2, 3, \ldots, 10$) and $\operatorname{cn}(\rho_n)\operatorname{dn}(\rho_n)\operatorname{sn}^j(\rho_n)$ ($j = 0, 1, 2, 3, \ldots, 10$) to zero. To avoid the tediousness, we omit the over-determined algebraic equations. From the algebraic equations, we found the important relations for the system parameters as

$$\beta = -\alpha, \qquad \gamma = s, \qquad \lambda = -\nu \quad \text{and} \quad \epsilon = -\sigma. \tag{27}$$

The above relations are obtained by different methods in [30, 31]. In [30] the authors have derived the periodic and Jacobi elliptic function solutions for the non-local DCCQGL equation by using the Hirota method. The initial amplitude of the solution is chosen arbitrarily and then the modulus of the Jacobi elliptic function is derived. However, the modulus of the Jacobi elliptic function is well known; it is between 0 and 1. So the determination of the atomic density of the condensate is not at all exact because the initial amplitude of the solution is arbitrary. In this paper, we derived the Jacobi elliptic function and solitary wave solutions for the nonlocal DCCQGL equation by using the extended Jacobi elliptic function approach. The method of approach and form of our solution is entirely different from that in [30], where we are quite sure about its complete novelty. Our aim is to calculate the atomic density of the condensate. For this reason, we have derived the Jacobi elliptic solutions with the exact determination of the initial amplitudes μ_1 and μ_2 (see equation (25)) as a function of the system parameters and modulus of the Jacobi elliptic function m. Therefore, the amplitude of periodic and solitary wave solutions can be calculated exactly to give the total number of atoms in the condensates. Under these parametric conditions (27), we solve the remaining algebraic equations. From our detailed analysis, we have found that the exact solution is possible only if the real and imaginary part of the system parameters satisfy the conditions (27). Thus, with the help of above system parameter conditions, we have obtained the new form of exact periodic and soliton solutions for equation (2) as follows.

3.1. Simple sn and kink soliton solutions

In this subsection, we find the periodic sn and kink soliton solutions of equation (2). To proceed further, we set the parameter values $c = 0$, $\mu_0 = \mu_2 = 0$ and $r = 0$; then, we obtain $s = 2\alpha[\operatorname{cn}(u)\operatorname{dn}(u) - 1]$. Using these physical parameter values, the new type of simple *sn* periodic solution is found to be

$$\psi_n^{(1)} = \pm m \operatorname{sn}(u) \left[\frac{\sigma \pm \sqrt{\sigma^2 + 4\alpha\nu \operatorname{cn}^2(u)\operatorname{dn}^2(u)}}{2\nu \operatorname{cn}(u)\operatorname{dn}(u)} \right]^{1/2} \operatorname{sn}(un + \delta_1)\, \mathrm{e}^{\mathrm{i}[2\alpha[\operatorname{cn}(u)\operatorname{dn}(u)-1]t+\delta_2]}. \tag{28}$$
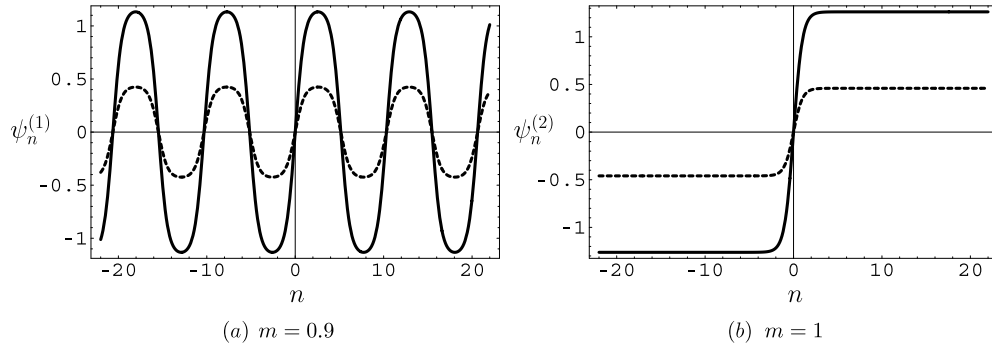
Figure 5. The simple sn and kink soliton solution for equation (2). (*a*) Periodic sn solution. (*b*) Kink soliton solution. Other physical parameters are $r = 0$, $t = 0$, $u = 1$, $\alpha = 1$, $\nu = 1$ and $\delta_1 = \delta_2 = 0$. In both figures, the solid and dashed lines correspond to repulsive ($\sigma = 1$) and attractive ($\sigma = -1$) condensates, respectively.

The parameter δ_1 in equation (28) defines the position of the solution. When $\delta_1 = 0$, the center of the solution coincides with the lattice site, which means that the solution is symmetric. Moreover, for the value of $\delta_1 \neq 0$, the solution is asymmetric because the center of the solution is located between the lattice sites. The parameter δ_2 in equation (28) is an arbitrary constant. Figure 5(*a*) portrays the properties of the simple sn solution of equation (2) when $r = 0$. Other physical parameters are $m = 0.9$, $u = 1$, $\alpha = 1$, $\nu = 1$ and $\delta_1 = \delta_2 = 0$. As observed in figure 5(*a*), the solid line corresponds to the sn solution of the repulsive condensate when $\sigma = 1$ and the dashed line represents the sn solution of the attractive condensate when $\sigma = -1$. Substituting the modulus of the Jacobi elliptic function $m = 1$ in equation (28), we obtain a new type of kink soliton solution of equation (2) which is given as follows:

$$\psi_n^{(2)} = \pm \tanh(u) \left[\frac{\sigma \pm \sqrt{\sigma^2 + 4\alpha\nu \, \mathrm{sech}^4(u)}}{2\nu \, \mathrm{sech}^2(u)} \right]^{1/2} \tanh(un + \delta_1) \, \mathrm{e}^{\mathrm{i}[2\alpha(\mathrm{sech}^2(u)-1)t+\delta_2]}. \quad (29)$$

The properties of the kink soliton solution is shown in figure 5(*b*). As plotted in figure 5(*b*), the solid and dashed lines correspond to the kink soliton solution for repulsive ($\sigma = 1$) and attractive ($\sigma = -1$) condensates, respectively.

3.2. Simple sn^2 and bubble soliton solutions

In order to discuss the next interesting case for the exact periodic and soliton solutions, we consider $c = 0$, $\mu_0 = \mu_1 = 0$ and $r = 0$. Then, we have the value $s = 2\alpha[\mathrm{cn}^2(u) \, \mathrm{dn}^2(u) - 1]$. According to these conditions, the simple sn^2 periodic solution of equation (2) can be written as

$$\psi_n^{(3)} = \pm m^2 \sqrt{\frac{2\alpha}{\sigma}} \, \mathrm{sn}^2(u) \, \mathrm{cn}(u) \, \mathrm{dn}(u) \, \mathrm{sn}^2(un + \delta_1) \, \mathrm{e}^{\mathrm{i}[2\alpha[\mathrm{cn}^2(u) \, \mathrm{dn}^2(u)-1]t+\delta_2]}. \quad (30)$$

This sn^2 solution of equation (2) exists only when the following two conditions are satisfied: (i) $\sigma > 0$, $\alpha > 0$, and (ii) $\sigma < 0$, $\alpha < 0$. These conditions also exist for the bubble soliton solution of equation (2) when $m = 1$. Figure 6(*a*) depicts the sn^2 solution for the attractive
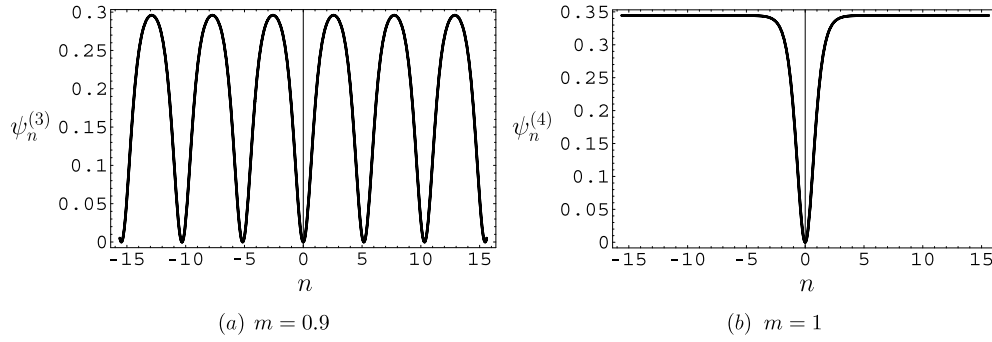
11

(a) $m = 0.9$　　　　　　　　　　　(b) $m = 1$

Figure 6. The plots for the simple sn^2 and bubble soliton solutions of the DCCQGL equation. (a) Periodic sn^2 and (b) bubble soliton solutions for attractive condensate when $\sigma = -1, \alpha = -1$. Other physical parameter values are $r = 0, t = 0, u = 1, v = 1$ and $\delta_1 = \delta_2 = 0$. The same plots are obtained for repulsive condensates when $\sigma = 1, \alpha = 1$.

condensate when $\sigma = -1$ and $\alpha = -1$. In addition, we obtain the same plot for the repulsive condensate when $\sigma = 1$ and $\alpha = 1$. From solution (30), we obtain a new type of bubble soliton solution of equation (2), when $m = 1$, given as

$$\psi_n^{(4)} = \pm\sqrt{\frac{2\alpha}{\sigma}}\ \tanh^2(u)\,\mathrm{sech}^2(u)\,\tanh^2(un + \delta_1)\ \mathrm{e}^{\mathrm{i}[2\alpha(\mathrm{sech}^4(u)-1)t+\delta_2]}. \tag{31}$$

The above solution (31) is called the new form of the bubble soliton solution of equation (2). The conditions for the bubble soliton are also mentioned in this section. The properties of bubble soliton solutions are shown in figure 6(b).

3.3. Alternating phase sn and kink soliton solutions

In contrast to the above studies, here we consider the parameter values as $c = 0$, $\mu_0 = \mu_2 = 0$, $r = \pi$; then, we find $s = -2\alpha[\mathrm{cn}(u)\,\mathrm{dn}(u)+1]$. Using these parameter values, the alternating phase sn solutions of the DCCQGL equation can be written as

$$\psi_n^{(5)} = \pm m(-1)^n\,\mathrm{sn}(u)\left[\frac{-\sigma \pm \sqrt{\sigma^2 + 4\alpha v\,\mathrm{cn}^2(u)\,\mathrm{dn}^2(u)}}{2v\,\mathrm{cn}(u)\,\mathrm{dn}(u)}\right]^{1/2}$$
$$\times\ \mathrm{sn}(un + \delta_1)\,\mathrm{e}^{\mathrm{i}[-2\alpha(\mathrm{cn}(u)\,\mathrm{dn}(u)+1)t+\delta_2]}. \tag{32}$$

Figure 7(a) shows the properties of the alternating phase sn solution of equation (2) when $r = \pi$. Figure 7(a) represents the alternating phase sn solution for the repulsive ($\sigma = 1$) condensate as indicated by the thick line and thin line for the attractive case ($\sigma = -1$). Substituting the modulus of the Jacobi elliptic function $m = 1$ in equation (32), we obtain a new type of alternating phase kink soliton solution of equation (2), when $r = \pi$, given by

$$\psi_n^{(6)} = \pm(-1)^n\,\tanh(u)\left[\frac{-\sigma \pm \sqrt{\sigma^2 + 4\alpha v\,\mathrm{sech}^4(u)}}{2v\,\mathrm{sech}^2(u)}\right]^{1/2}$$
$$\times\ \tanh(un + \delta_1)\,\mathrm{e}^{\mathrm{i}[-2\alpha(\mathrm{sech}^2(u)+1)t+\delta_2]}. \tag{33}$$

The properties of alternating phase kink soliton solutions are displayed in figure 7(b). In figure 7(b), the thick line corresponds to the soliton solution of the repulsive condensate when
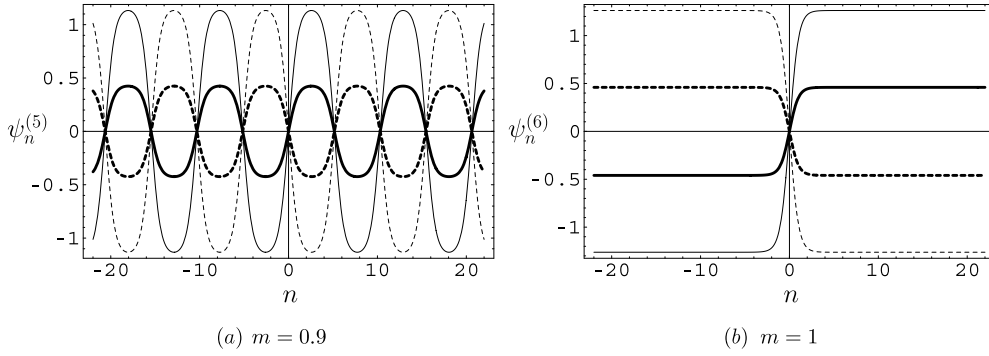
(*a*) $m = 0.9$ (*b*) $m = 1$

Figure 7. The alternating phase sn and kink soliton solutions of the DCCQGL equation. (*a*) The alternating phase sn solution when $m = 0.9$. (*b*) The alternating phase kink soliton when $m = 1$. Other physical parameters are $t = 0$, $r = \pi$, $u = 1$, $\alpha = 1$, $\nu = 1$ and $\delta_1 = \delta_2 = 0$. In both figures, the thick and thin lines represent the repulsive ($\sigma = 1$) and attractive ($\sigma = -1$) condensates, respectively.

$\sigma = 1$ and the thin line represents the soliton solution of the attractive condensate when $\sigma = -1$.

3.4. Alternating phase sn^2 and bubble soliton solutions

Finally, we consider the parameter values as $c = 0$, $\mu_0 = \mu_1 = 0$, $r = \pi$. Then, we obtain $s = -2\alpha[\text{cn}^2(u)\,\text{dn}^2(u) + 1]$. With the help of these parameter values, the alternating phase sn^2 solution of equation (2) is given by

$$\psi_n^{(7)} = \pm m^2(-1)^n\sqrt{\frac{-2\alpha}{\sigma}}\,\text{sn}^2(u)\,\text{cn}(u)\,\text{dn}(u)\,\text{sn}^2(un + \delta_1)\text{e}^{\text{i}[-2\alpha(\text{cn}^2(u)\,\text{dn}^2(u)+1)t+\delta_2]}. \tag{34}$$

The alternating phase sn^2 solution exists if the following two physical conditions are satisfied: (i) $\sigma > 0$, $\alpha < 0$, and (ii) $\sigma =< 0$, $\alpha > 0$. Figure 8(*a*) shows the alternating phase sn^2 solution for the attractive condensate when $\sigma = -1$ and $\alpha = 1$. Further, we obtain the same plot for the repulsive condensate when $\sigma = 1$ and $\alpha = -1$. When the modulus of the Jacobi elliptic function is equal to 1, the exact alternating phase bubble soliton solution is found to be

$$\psi_n^{(8)} = \pm(-1)^n\sqrt{\frac{-2\alpha}{\sigma}}\,\tanh^2(u)\,\text{sech}^2(u)\,\tanh^2(un + \delta_1)\,\text{e}^{\text{i}[-2\alpha(\text{sech}^4(u)+1)t+\delta_2]}. \tag{35}$$

The two above-mentioned conditions also exist for the alternating phase bubble soliton solution. The properties for the alternating phase bubble soliton solution for attractive ($\sigma = -1$ and $\alpha = 1$) condensates is shown in figure 8(*b*). We have also generated the same plot for the repulsive condensate when $\sigma = 1$ and $\alpha = -1$.

In the system of BECs, the atomic density of periodic and solitary wave solutions is defined by $N_{ad} = \left|\psi_n^{(j)}\right|^2$ ($j = 1, 2, \ldots, 8$). The atomic density of the condensate is a conserved quantity whose determination is very much needed in the study of BECs. These amplitudes are determined by the system parameters and modulus of the Jacobi elliptic function. From these periodic and solitary wave solutions, one can exactly calculate the atomic density of the condensates. When we fix the system parameter, the amplitude of the solution can only be changed by varying the modulus parameter m. Therefore, these solutions will be more helpful for BEC experiments in the near future. The predicted feature of our results could be possibly
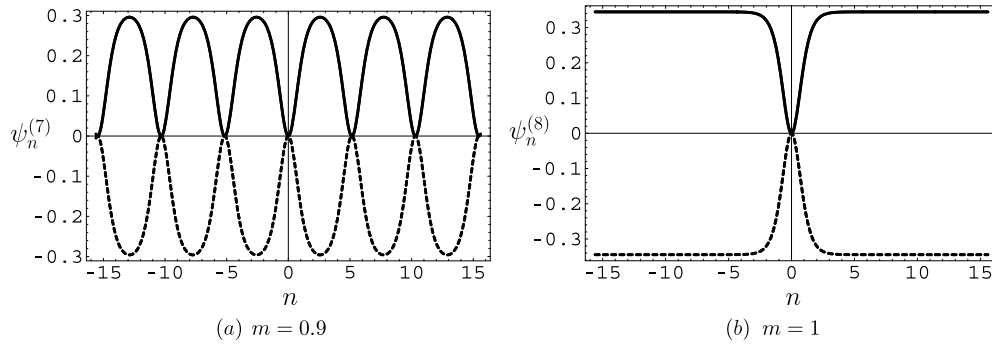
Figure 8. The alternating phase sn^2 and bubble soliton solutions of equation (2). (*a*) The alternating phase sn^2 and (*b*) alternating phase bubble soliton solutions for the attractive condensates when $\sigma = -1$ and $\alpha = 1$. Other physical parameter values are $t = 0$, $r = \pi$, $u = 1$, $v = 1$ and $\delta_1 = \delta_2 = 0$. The same plots are obtained for repulsive condensates when $\sigma = 1$ and $\alpha = -1$.

observed in experimental settings for the BEC in optical lattice. To the best of our knowledge, the BEC in optical lattice is closely related to the most actual challenges of the modern atom optics, namely developing the atomic chip and atomic waveguides. As regards their intrinsic interest, lattice solitons have many potential applications in atomic interferometry and matter-wave lasers.

4. Conclusion

In conclusion, we have investigated the modulational instability in a system of BECs in a deep optical lattice, which is described by the discrete complex cubic–quintic Ginzburg–Landau equation with the non-local quintic term. We have obtained the characteristics of the modulational instability in the form of typical dependences of the instability growth rate (gain) on the perturbation wavenumber and the system's parameters. Numerical studies have corroborated our analytical findings. By using the extended Jacobi elliptic function approach, we have found a set of periodic and new type of solitary wave solutions for the considered system. These solutions consist of simple Jacobi elliptic functions and alternating phase Jacobi elliptic function solutions. Also, we have given the new type of kink and bubble soliton solutions, alternating phase kink and bubble soliton solutions when the modulus of the Jacobi elliptic function is set to be 1. These new forms of periodic and solitary wave solutions and related properties are not only applicable in the BEC but also in many physical systems such as nonlinear optics, phase transition, non-equilibrium systems, superconductivity and superfluidity.

Appendix

The coefficients of the 2×2 matrix (m_{ij}) of equation (10) are

$$m_{11} = (\epsilon + i\sigma)A^2 + 2(\beta + i\alpha)\cos(q)\{\cos(Q) - 1\} + 2(\lambda + i\nu)A^4$$
$$\times \cos(q)\{\cos(Q) + 1\} - 2[\beta + i\alpha + (\lambda + i\nu)A^4]\sin(q)\sin(Q), \tag{A.1}$$

$$m_{12} = (\epsilon + i\sigma)A^2 + 4(\lambda + i\nu)A^4\cos(q), \tag{A.2}$$

$$m_{21} = (\epsilon - i\sigma)A^2 + 4(\lambda - i\nu)A^4\cos(q), \tag{A.3}$$

$$m_{22} = (\epsilon - i\sigma)A^2 + 2(\beta - i\alpha)\cos(q)\{\cos(Q) - 1\} + 2(\lambda - i\nu)A^4$$
$$\times \cos(q)\{\cos(Q) + 1\} + 2[\beta - i\alpha + (\lambda - i\nu)A^4]\sin(q)\sin(Q). \tag{A.4}$$

References

[1] Aranson I S and Kramer L 2002 *Rev. Mod. Phys.* **74** 99
    Malomed B A 2005 *Encyclopedia of Nonlinear Science* ed A Scott (New York: Routledge)
[2] Hocking L M and Stewartson K 1972 *Proc. R. Soc.* A **326** 289
    Pereira N R and Stenflo L 1977 *Phys. Fluids* **20** 1733
[3] Petviashvili V I and Sergeev A M 1984 *Dokl. Akad. Nauk SSSR* **276** 1380
    Petviashvili V I and Sergeev A M 1984 *Sov. Phys. Doklady* **29** 493
[4] Malomed B A 1987 *Physica* D **29** 155
[5] Van Saarloos W and Hohenberg P C 1990 *Phys. Rev. Lett.* **64** 749
    Malomed B A and Nepomnyashchy A A 1990 *Phys. Rev.* A **42** 6009
    Hakim V, Jakobsen P and Pomeau Y 1990 *Europhys. Lett.* **11** 19
    Marcq P, Chaté H and Conte R 1994 *Physica* D **73** 305
    Soto-Crespo J M, Akhmediev N N and Afanasjev V V 1996 *J. Opt. Soc. Am.* B **13** 1439
[6] Trombettoni A and Smerzi A 2001 *Phys. Rev. Lett.* **86** 2353
    Abdullaev F Kh, Tsoy E N, Malomed B A and Kraenkel R A 2003 *Phys. Rev.* A **68** 053606
    Ahufinger V, Sanpera A, Pedri P, Santos L and Lewenstein M 2004 *Phys. Rev.* A **69** 053604
[7] Eisenberg H S, Silberberg Y, Morandotti R, Boyd A and Aitchison J S 1998 *Phys. Rev. Lett.* **81** 3383
    Bang O and Miller P 1996 *Opt. Lett.* **21** 1105
    Morandotti R, Peschel U, Aitchison J S, Eisenberg H S and Silberberg Y 1999 *Phys. Rev. Lett.* **83** 2726
    Ablowitz M and Musslimani Z H 2001 *Phys. Rev. Lett.* **87** 254102
    Sukhorukov A A and Kivshar Y 2002 *Phys. Rev.* E **65** 036609
    Peschelb U, Morandotti R, Arnold J M, Aitchison J S, Eisenberg H S, Silberberg Y, Pertsch T and Lederer F
      2002 *J. Opt. Soc. Am.* B **19** 2637
    Ablowitz M J and Musslimani Z H 2002 *Phys. Rev.* E **65** 056618
    Fleischer J W, Carmon T, Segev M, Efremidis N K and Christodoulides D N 2003 *Phys. Rev. Lett.* **90** 023902
[8] Su W P, Schieffer J R and Heeger A J 1979 *Phys. Rev. Lett.* **42** 1698
    Liu Y, Bartal G, Genov D A and Zhang X 2007 *Phys. Rev. Lett.* **99** 153901
[9] Christodoulides D N and Efremidis N K 2002 *Opt. Lett.* **27** 568
    Efremidis N K, Sears S, Christodoulides D N, Fleischer J W and Segev M 2002 *Phys. Rev.* E **66** 046602
[10] Fleischer J W, Segev M, Efremidis N K and Christodoulides D N 2003 *Nature* **422** 147
    Chen Z, Martin H, Eugenieva E D, Xu J and Yang J 2005 *Opt. Exp.* **13** 1816
[11] Flach S and Willis C R 1998 *Phys. Rep.* **295** 181
    Fleurov V 2003 *Chaos* **13** 676
    Morsch O and Oberthaler M 2006 *Rev. Mod. Phys.* **78** 179
    Flach S and Gorbach A V 2008 *Phys. Rep.* **467** 1
[12] Abdullaev F Kh, Baizakov B B, Darmanyan S A, Konotop V V and Salerno M 2001 *Phys. Rev.* A **64** 043606
    Brazhnyi V A and Konotop V V 2004 *Mod. Phys. Lett.* B **18** 627
    Alfimov G, Kevrekidis P G, Konotop V V and Salerno M 2002 *Phys. Rev.* E **66** 046608
[13] Tiofack G C L, Mohamadou A and Kofané T C 2007 *J. Phys. A: Math. Theor.* **40** 6133
[14] Willaime H, Cardoso O and Tabeling P 1991 *Phys. Rev. Lett.* **67** 3247
    Wang S S and Winful H G 1988 *Appl. Phys. Lett.* **52** 1774
    Otsuka K 1990 *Phys. Rev. Lett.* **65** 947

[15] Maruno K, Ankiewicz A and Akhmediev N 2003 *Opt. Commun.* **221** 199
[16] Leo X and Hai W 2005 *Chaos* **15** 033702
     Marklund M and Shukla P K 2005 *Eur. Phys. J.* B **48** 71
[17] Abdullaev F Kh, Bouketir A, Messikh A and Umarov B A 2007 *Physica* D **232** 54
[18] Wamba E, Mohamadou A and Kofané T C 2008 *Phys. Rev.* E **77** 046216
[19] Zhang W, Wright E M, Pu H and Meystre P 2003 *Phys. Rev.* A **68** 023605
[20] Filho V S, Gammal A, Frederico T and Tomio L 2000 *Phys. Rev.* A **62** 033605
     Adhikari S K 2002 *Phys. Rev.* A **66** 043601
     Muruganandam P and Adhikari S K 2002 *Phys. Rev.* A **65** 043608
[21] Mohamadou A and Kofané T C 2006 *Phys. Rev.* E **73** 046607
     Mohamadou A, Tiofack G C L and Kofané T C 2006 *Phys. Scr.* **74** 718
[22] Abdullaev F Kh, Abdumalikov A A and Umarov B A 2002 *Phys. Lett.* A **305** 371
[23] Efremidis N K and Christodoulides D N 2003 *Phys. Rev.* E **67** 026606
[24] Greiner M, Mandel O, Esslinger T, Haensch J W and Bloch I 2002 *Nature* **415** 39
     Schmidt K P, Dorier J, Läuchli A and Mila F 2006 *Phys. Rev.* B **74** 174508
     Huhtamäki J A M, Möttönwn M, Ankerhold J and Virtanen S M M 2007 *Phys. Rev.* A **76** 033605
[25] Anderson B P and Kasevich M A 1998 *Science* **282** 1686
[26] Abdullaev F Kh, Gammal A, Tomio L and Frederico T 2001 *Phys. Rev.* A **63** 043604
[27] Christodoulides D N and Joseph R I 1988 *Opt. Lett.* **13** 794
[28] Akhmediev N and Ankiewicz A 2001 *Spatial Solitons* ed S Trillo and W E Toruellas (Berlin: Springer)
     pp 311–42
     Moores J D 1993 *Opt. Commun.* **96** 65
[29] Akhmediev N, Das M P and Vagov A V 1999 *Int. J. Mod. Phys.* B **13** 625
[30] Maruno K, Ankiewicz A and Akhmediev N 2005 *Phys. Lett.* A **347** 231
[31] Dai C and Zhang J 2006 *Opt. Commun.* **263** 309
[32] Descalzi O 2005 *Phys. Rev.* E **72** 046210
     Descalzi O and Brand H R 2005 *Phys. Rev.* E **72** 055202
[33] Cross M C and Hohenberg P C 1993 *Rev. Mod. Phys.* **65** 851
[34] Manneville P 1990 *Dissipative Structures and Weak Turbulence* (San Diego, CA: Academic)
[35] Kuramoto Y 1984 *Chemical Oscillations, Waves and Turbulence* (Berlin: Springer)
[36] Akhmediev N and Ankiewicz A 1997 *Solitons, Nonlinear Pulses and Beams* (London: Chapman and Hall)
[37] Nicolis G 1995 *Introduction to Nonlinear Science* (Cambridge: Cambridge University Press)
[38] Zhang A X and Xue J K 2008 *Phys. Lett.* A **372** 1147
[39] Mohamdou A, Jiotsa A K and Kofané T C 2005 *Phys. Rev.* E **72** 036220
[40] Rapti Z, Kevrekidis P G, Smerzi A and Bishop A R 2004 *J. Phys. B: At. Mol. Opt. Phys.* **37** S257
[41] Kivshar Y S and Peyrard M 1992 *Phys. Rev.* A **46** 3198